Anomeric Specificity of D-Xylose Isomerase[†,‡]

C. A. Collyer,[§,∥] J. D. Goldberg,[∥] H. Viehmann, D. M. Blow,[*,∥] N. G. Ramsden,[⊥] G. W. J. Fleet,[⊥] F. J. Montgomery,[#] and P. Grice[#]

Blackett Laboratory, Imperial College, London SW7 2BZ, Dyson Perrins Laboratory, Oxford University, Oxford OX1 3QY, and Whiffen Laboratory, Imperial College, London SW7 2AZ

Received October 9, 1991; Revised Manuscript Received June 17, 1992

ABSTRACT: Crystal structures of complexes of D-xylose isomerase with deoxysugars have been determined. Deoxynojirimycin is a structural analogue of α-pyranose and mimics the binding of these aldose substrates. The structure of this complex supports the hypothesis that an imidazole group catalyzes ring opening of the pyranose. The steric restrictions in the active site of the enzyme prevent a β-pyranose from binding in the same way. For the reverse reaction with ketoses, the anomeric specificity is less certain. Dideoxyimino-D-glucitol is a structural analogue of the ketose α-D-furanose. The binding of the inhibitor dideoxyimino-D-glucitol to the crystals of the enzyme does not mimic the binding of the reactive α-D-fructofuranose. Superposition of the nonphysiological substrate α-D-fructofuranose onto the atomic positions of dideoxyimino-D-glucitol is not possible due to the steric restrictions of the active site. However, by utilizing the approximate 2-fold symmetry of the sugar, a stereochemically sensible model is produced which is consistent with other data. In addition to reaction with α-D-furanose, the enzyme probably reacts with open ring keto sugars which are present at significant concentrations. Other sugars which resemble furanoses either do not inhibit significantly or are not observed in the crystals bound in a single conformation.

The D-xylose to D-xylulose interconverting enzyme, D-xylose ketol isomerase (EC 5.3.1.5), also interconverts D-glucose and D-fructose and is primarily used by industry for the production of high-fructose corn syrups. Protein engineering of D-xylose isomerase (Batt et al., 1989; Lee et al., 1990; Meng et al., 1991) has been guided by knowledge of crystallographically determined substrate and inhibitor binding states (Henrick et al., 1989; Carrell et al., 1989; Collyer et al., 1990; Whitlow et al., 1991). A key element in this work is the anomeric specificity of the enzyme toward its sugar substrates.

Enzymes may bind and react with only some of the anomeric forms of their sugar substrates found in solution. The reactive anomers of the aldose substrates of D-xylose isomerase are the α-pyranose forms of D-xylose and D-glucose (Feather et al., 1970; Schray & Rose, 1971; Schray & Mildvan, 1972; Young et al., 1975; McKay & Tavlarides, 1979). α-D-Glucopyranose is observed as the primary product for D-fructose to D-glucose conversion (Bock et al., 1983; Makkee et al., 1984). This is consistent with the observations in crystal structures of complexes of the enzyme with 5-thio-α-D-glucopyranose (Collyer et al., 1990) and α-D-xylopyranose (Whitlow et al., 1991).

The reactivity of the various anomeric forms of ketoses towards D-xylose isomerase is not so well known. Similar studies with D-xylose isomerase for ketoses are complicated by the rapid interconversion of α- and β-D-fructofuranoses (Goux, 1985). On initial reaction with D-glucose, Bock et al. (1983) observe the formation of a higher than equilibrium proportion of β-D-fructofuranose relative to total D-fructose. Because of the fast mutarotation rate at 65 °C between α- and β-D-fructofuranoses, this accumulation of β-D-fructofuranose could result from enzymatic production of either of the D-fructofuranoses. Makkee et al. (1984) have followed the enzymatic reaction with [1-^{13}C]D-glucose by ^{13}C NMR and reported the formation of an initial higher than equilibrium ratio of α-D-fructofuranose anomer to β-D-fructofuranose anomer. These data indicate that at least some of the reacting species are α-D-furanose forms.

Two divalent metal cations are observed bound at the active site of the enzyme, and both are believed to be essential for activity. The cation at site 1 binds and orients the sugars while cation 2 is directly involved in the isomerization reaction. A basic solvent molecule (Wat519) in the coordination sphere of divalent cation 2 is within hydrogen-bonding distance of the sugar oxygens and is implicated in the reaction mechanism. Keto or aldehydo open ring forms of the substrates are observed crystallographically bound to the active site of the enzyme (Collyer et al., 1990; Whitlow et al., 1991), indicating that they are reactive species or intermediates in the reaction (Collyer & Blow, 1990; Lee et al., 1990).

The conservation of active site residues (Henrick et al., 1989) and close correspondence of structures of crystallographically determined D-xylose isomerases (Henrick et al., 1987) confirms the general relevance of studies of these enzymes from diverse sources. We have studied the binding and the crystallographic structures of the complexes of *Arthrobacter* D-xylose isomerase with compounds which are stereochemically similar to substrates. These structures can then be analyzed for an understanding of the anomeric specificity.

[†] This research was funded by the Molecular Recognition Initiative of the Science and Engineering Research Council, in the U.K.

[‡] The refined coordinates have been submitted to the Brookhaven Protein Data Bank.

[*] Author to whom correspondence should be addressed.

[§] Present address: Research & Development, Farmitalia Carlo Erba, Nerviano, Lombardy, Italy.

[∥] Blackett Laboratory, Imperial College.

[⊥] Oxford University.

[#] Whiffen Laboratory, Imperial College.

0006-2960/92/0431-12211$03.00/0 © 1992 American Chemical Society

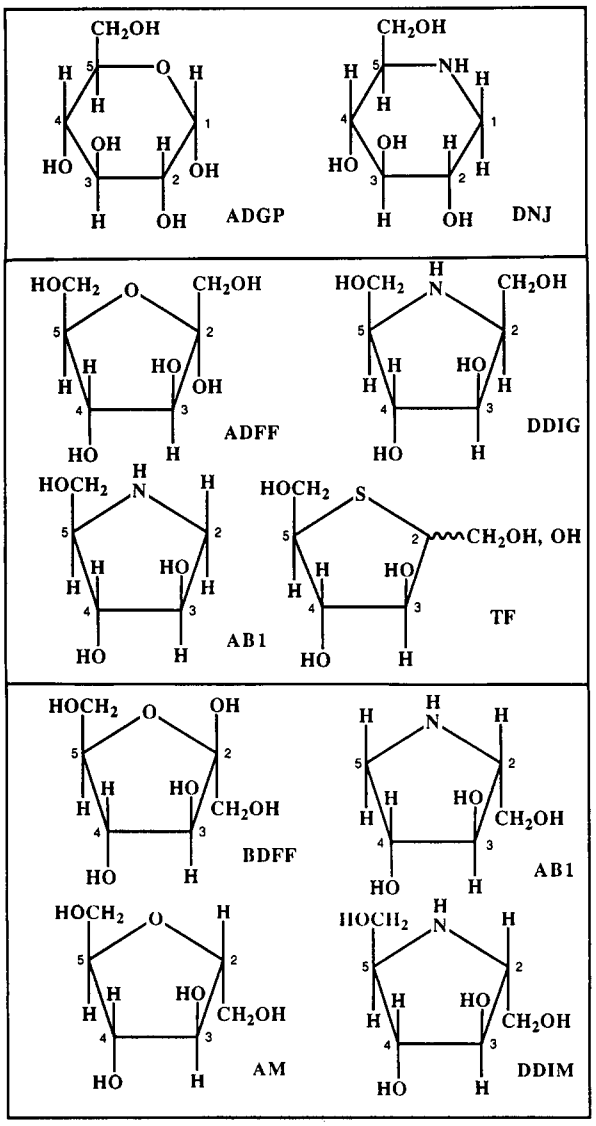

FIGURE 1: Comparison of compounds with putative substrates of D-xylose isomerase; abbreviations are as defined: (a, top) α-D-glucopyranose (ADGP) and 1-deoxynojirimycin (DNJ); (b, middle) α-D-fructofuranose (ADFF), 2,5-dideoxy-2,5-imino-D-glucitol (DDIG), 1,4-dideoxy-1,4-imino-D-arabinitol (AB1), and 5-thio-D-fructose (TF); (c, bottom) β-D-fructofuranose (BDFF), 1,4-dideoxy-1,4-imino-D-arabinitol (AB1), 2,5-anhydro-D-mannitol (AM), and 2,5-dideoxy-2,5-imino-D-mannitol (DDIM).

EXPERIMENTAL PROCEDURES

Materials. The D-xylose isomerase enzyme (EC 5.3.1.5) from *Arthrobacter* strain B3728 was prepared as previously (Smith et al., 1991; Akins et al., 1986). The metal-free enzyme was stored at 20–30 mg/mL under liquid nitrogen.

DNJ (1-deoxynojirimycin) (Inouye et al., 1968) was supplied as a gift by Bayer AG. AB1 (1,4-dideoxy-1,4-imino-D-arabinitol) (Wyn et al., 1985) was a gift from Dr. R. Nash, (Nash et al., 1985). The DDIG (2,5-dideoxy-2,5-imino-D-glucitol) (Reitz & Baxter, 1990) and the DDIM (2,5-dideoxy-2,5-imino-D-mannitol) (Fleet & Smith, 1985) were prepared from glucose (N. G. Ramsden, A. J. Fairbanks, G. W. J. Fleet, I. Cenci di Bello, B. Winchester, and J. D. Goldberg, unpublished results). TF (5-thio-D-fructose) was synthesized by the procedure of Chmielewski and Whistler (1975) starting from (1,2-*o*-isopropylidene-α-L-sorbose) (Patil & Bose, 1966). AM (2,5-anhydro-D-mannitol) was supplied by the Sigma Chemical Company. These substrate-like compounds are compared with sugars ADGP (α-D-glucopyranose), ADFF (α-D-fructofuranose), and BDFF β-D-fructofuranose (Figure 1).

Crystallographic Procedures. The crystal form of the *Arthrobacter* enzyme is in space group $P3_121$, $a = 106$ Å and $c = 154$ Å, with two subunits of the tetramer in the asymmetric unit (Akins et al., 1986). For crystal soaks, metal-free apocrystals were initially harvested into a 2.8 M ammonium sulfate solution, saturated with thymol and buffered to pH 7.8 with 50 mM triethanolamine. Crystals were subsequently transferred to similarly buffered solutions containing 3.2 M ammonium sulfate, divalent cation, inhibitor or sugar, and saturating thymol. Following soaks of at least 40 h, crystals were mounted in the capilliary tube, and a small quantity of solid thymol was inserted to ensure saturating conditions.

Data sets at 2.5-Å resolution were recorded on film at the synchrotron radiation source, Daresbury, as previously described (Henrick et al., 1989). Subsequent processing and reduction of the data was carried out using the CCP4 suite of programs.[1] For all data sets, an initial model was constructed by removing the inhibitor and water molecules from the active site of a model previously refined by Henrick et al. (1989) and Collyer et al. (1990). The choice of starting model was determined by the correspondence between the sets of observed diffraction intensities. Calculation of difference electron density maps (Fourier coefficients $F_o - F_c$) allowed manual improvement of starting models, but crystals of different derivatives in this crystal form are slightly nonisomorphous, due to rotation and translation of the tetramers relative to the crystallographic 2-fold axis passing through them (Collyer et al., 1990). For refinement of these models, the restrained least-squares refinement program PROLSQ (Hendrickson & Konnert, 1980) was alternated with rounds of manual intervention. Refinement proceeded for all models until all uninterpretable difference electron density was less than 4 times the rms deviation from mean density. The difference electron density maps shown in Figures 2 and 4 are computed after refinement. Contour levels in these maps are chosen to reflect the different signal to noise levels, which are related to the average refined temperature factors of the different inhibitors.

Modeling. In modeling the substrate interactions, a hydrogen bond is assumed between substrate oxygens and O or N atoms of the enzyme, when appropriate stereochemistry exists and when the refined coordinates indicate a distance not exceeding 3.2 Å. Atoms are considered to coordinate the active site cations if they are within 2.7 Å or less.

D-Xylose Isomerase Assay. For determination of inhibition constants, D-xylose isomerase activity was assayed with D-fructose as substrate (Smith et al., 1991). A substrate solution containing D-fructose (88 or 175 mM), $MgCl_2$ (10 mM), Tris-HCl (50 mM, pH 7.95), and inhibitor was preincubated at 20 °C for 20 min. A 3.75 mg/mL solution of D-xylose isomerase was preincubated in the same manner in the presence of $MgCl_2$ (10 mM) and Tris-HCl (50 mM, pH 7.95). The reaction was initiated by the addition of 7 μL of the enzyme solution to 50 μL of substrate solution. The reaction was stopped by the rapid addition of a 16-μL aliquot of the reaction mixture to an equal volume of 15% (w/v) trichloroacetic acid. The amount of glucose formed was determined by spectrophotometric assay using a commercial diagnostic kit (GOD-PERID reagent kit supplied by Boehringer Corp. Ltd.).

[1] The SERC (U.K.) Collaborative Computing Project No. 4, a Suite of Programs for Protein Crystallography, distributed from Daresbury Laboratory, Warrington WA4 4AD, U.K.

Table I: Diffraction Data

data set	DNJ	DDIG
metal soak	Mg^{2+}	Mn^{2+}
concentration (mM)	200	50
inhibitor	1-deoxy-nojirimycin	2,5-dideoxy-2,5-imino-D-glucitol
concentration (mM)	550	1000
pH	8.0	7.8
temp (°C)	−10	21
a (Å)	105.6	106.1
c (Å)	153.4	153.3
resolution (Å)	2.55	2.5
N_{total}	72 882	72 763
N_{unique}	32 571	33 679
no. of crystals	1	1
data to res. (%)	96.4	95.8
R_{merge} (%)[a]	6.0 (18.2)	8.2 (15.7)

[a] Merging R factor:

$$R_{merge} = \frac{\sum_h \sum_i |I_{h,i} - \bar{I}_h|}{\sum_h \sum_i I_{h,i}}$$

The overall value is given, followed by the value for the outermost shell of data in parentheses.

Table II: Statistics for Refined Crystallographic Models

Rms Deviations from Ideal Geometry for the Final Models	DNJ	DDIG
distances (Å)		
bonds (1–2 neighbor) (0.025)[a]	0.019	0.019
angles (1–3 neighbor) (0.040)	0.046	0.048
planar groups (Å) (0.020)	0.013	0.015
nonbonded contacts (Å)		
single torsion (0.20)	0.16	0.17
multiple torsion (0.20)	0.18	0.22

R Factor for the Crystallographic Models	*R* factor (%)	
resolution (Å) (10.0 – res)	15.1 (DNJ)	14.9 (DDIG)
no. of reflections	31 966	33 272
no. of atoms	6659	6584
average B (Å^2)	22.0	24.7

[a] The values in parentheses are the input estimates of standard deviations that determine the relative weights of the corresponding geometric restraints (Hendrickson & Konnert, 1980).

RESULTS

Agreement of Crystallographic Data and Models. The conditions and results for diffraction data collection are summarized in Table I. Least-squares refinement gave crystallographic *R* factors of about 15–16% for all models, with the deviations from ideal geometry of the models (Table II) being comparable to the values previously obtained by Henrick et al. (1989).

The data sets presented here (Table I) and elsewhere (Henrick et al., 1989; Collyer et al., 1990) are not strictly isomorphous, and the differences in the diffraction intensities between the sets are significant. These differences are largely due to a small molecular rotation and translation within the crystal (Collyer et al., 1990). The overall accuracy of the refined crystallographic atomic models (Table II) may be estimated from the agreement between the two independent crystallographically refined monomers. The rms distance after superposition between the α-carbons of the two monomers in the asymmetric unit is 0.2 Å for models containing both DNJ and DDIG. The same rms distance of 0.2 Å is obtained after superposition between all the α-carbons of these two models. Less accuracy is expected for side-chain atoms and atoms of surface residues.

Deoxynojirimycin Complex. The analysis using DNJ was designed also to find whether Mg^{2+} could be bound at site 2. In view of the lower affinity of Mg^{2+} for this site, a high cation concentration was chosen (Table I), which was found to give full occupancy at site 2. Electron densities clearly indicate a bound state for DNJ in both crystallographically independent subunits (Figure 2). The mean refined temperature factors of 45 and 44 Å^2, respectively, are high and indicate thermal disorder or less than unit occupancy for the sugar. The binding is most similar to that reported previously for 5-thio-α-D-glucopyranose (Collyer et al., 1990) and α-D-xylopyranose (Whitlow et al., 1991). The sugar binds directly to His53 and via O3 and O4 to the cation at site 1 and its ligands (Table III). The imino group of DNJ is positioned close to His53 as observed for the sulfur of 5-thio-α-D-glucopyranose and is within hydrogen-bonding distance of the imidazole group (Figure 3).

In this structure, Mg^{2+} at site 2 and Asp254 are observed to be ordered. Mg^{2+} at site 2 has temperature factors of 22 and 17 Å^2, and a ligand to the cation, the side chain of Asp254, has temperature factors of 20 and 22 Å^2 for subunits A and B, respectively. The coordination appears distorted to pentacoordinate with a long distance observed to the imidazole of His219 (Table III).

Dideoxyiminoglucitol Complex. In the analysis using DDIG, Mn^{2+} was included, which binds at both sites with high affinity (Rangarajan & Hartley, 1992). The electron densities observed for the inhibitor DDIG indicate a bound state quite unlike that for the pyranoses (Figure 4). The mean refined temperature factors of 24 and 25 Å^2, respectively, are moderate and indicate close to unit occupancy. DDIG binds with the imino group and O6 as ligands to Mn^{2+} at site 1 (Table III). O6 forms a hydrogen bond to the water molecule of the hexa-coordinate Mn^{2+} at site 2. O1 forms a hydrogen bond with the carboxylate group of Asp244 and O4 hydrogen bonds to the imidazole of His53 (Figure 5a). This conformation has a number of similarities to that reported for a covalently bound methylene derivative of BDFF (Carrell et al., 1989).

In this DDIG-bound state the sidechain of Glu180 is ordered with mean refined temperature factors of 15 Å^2 for both subunits. This carboxylate side chain is a ligand to the cation at site 1. The observed conformation is, however, different from the "normal" conformation, that observed under all other conditions (Collyer et al., 1990; Whitlow et al., 1991). The difference between the DDIG-bound state and the "normal" state may be simply described as a substitution of one carboxylate oxygen by the other in the hexacoordinate sphere of the cation at site 1 (Figure 5b). The presence of O3 in DDIG and the "normal" conformation of Glu180 are mutually exclusive on steric grounds.

Uninterpretable Electron Densities. Two other experiments were performed for which the resulting electron densities at the active sites could not be interpreted. Crystals were soaked in saturated solutions of AB1 and TF (Figure 1), pH 7.8, with 50 mM Mn^{2+}, and X-ray diffraction data to 2.5-Å resolution, of similar quality to the DNJ and DDIG crystals, were recorded. After refinement these data sets gave models for the enzyme of the usual quality and clean difference maps except at the active site. Highly significant electron densities observed in the active site cavity could not be modeled by a single bound conformer of the sugar, nor could the densities be accounted for by solvent alone. The shape and width of the electron density were consistent with five-membered ring compounds, but the conformation(s) could not be determined

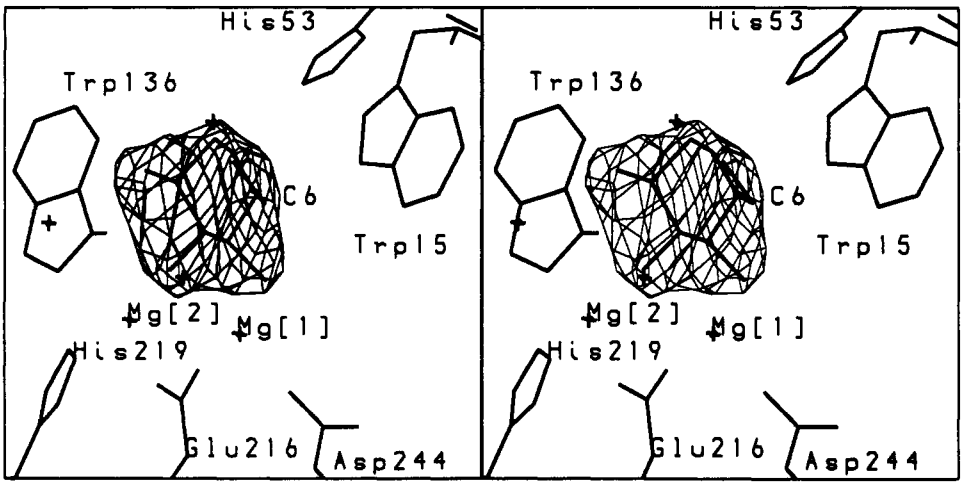

FIGURE 2: Stereodrawing of the electron density for the active site region of the DNJ–enzyme complex. The electron density is contoured at 5 times rms deviation (σ) from mean density and was calculated using Fourier coefficients ($F_o - F_c$). For the calculation of F_c and α, the coordinates of DNJ were omitted. The substrate and surrounding protein structure are shown using thick lines, and the unlabeled crosses are ordered solvent molecules. Density at O6 (not visible) is weak (3σ).

Table III: Possible Hydrogen Bonds and Metal Coordination Near the Substrate Binding Pocket for Crystallographic Independent Subunits A and B (Distances in Ångstroms)

		subunit A	subunit B			subunit A	subunit B
			Enzyme–Mg–DNJ Complex				
			(i) Magnesium, Coordination Site 1				
	Asp244–OD2	2.0	2.2		Asp292–OD1	2.0	2.2
	Glu180–OE2	2.4	2.3		inhibitor–O3	2.5	2.7
	Glu216–OE1	2.1	2.0		inhibitor–O4	2.1	1.9
			(ii) Magnesium, Coordination Site 2[a]				
	Asp254–OD1	2.0	2.3		Asp254–OD2	2.5	2.6
	Asp256–OD1	2.2	2.3		His219–NE2	3.0	3.0
	Glu216–OE2	1.9	2.0		Wat519	1.9	1.9
			(iii) Possible Hydrogen Bonds and Contacts between Inhibitor and the Enzyme				
inhibitor–O2	Wat487	3.0	2.8	inhibitor–O4	Glu180–OE2	3.2	2.7
	Wat518	2.8	3.1		Asp292–OD1	2.9	2.7
inhibitor–O3	Glu180–OE2	2.8	2.7		Asp244–OD2	3.2	2.9
	Glu216–OE1	3.0	3.1		Wat521	2.5	2.9
	Asp292–OD1	3.1	3.2	inhibitor–N5	His53–NE2	2.7	2.8
	Wat519	3.1	3.2	inhibitor–O6	His53–NE2	3.1	2.8
inhibitor–O4	Glu180–OE1	2.6	2.7		Wat520	2.8	2.6
			Enzyme–Mn–DDIG Complex				
			(i) Manganese, Coordination Site 1				
	Asp244–OD2	2.1	2.1		Asp292–OD1	2.0	2.0
	Glu180–OE1	2.2	2.1		inhibitor–N5	2.5	2.6
	Glu216–OE1	2.3	2.1		inhibitor–O6	2.4	2.5
			(ii) Manganese, Coordination Site 2				
	Asp254–OD1	2.2	2.3		Asp254–OD2	2.4	2.4
	Asp256–OD1	2.2	2.2		His219–NE2	2.6	2.5
	Glu216–OE2	2.1	2.1		Wat519	2.1	2.3
			(iii) Possible Hydrogen Bonds and Contacts between Inhibitor and the Enzyme				
inhibitor–O1	Asp244–OD1	2.8	2.8	inhibitor–O4	Wat520	3.0	2.8
inhibitor–O3	Glu180–OE1	2.9	3.0	inhibitor–O6	Wat519	2.6	2.9
inhibitor–O4	His53–NE2	2.8	3.1		Glu180–OE2	2.6	2.5

[a] The coordination is distorted from hexa- to pentacoordinate. This difference between Mn^{2+} and Mg^{2+} binding at site 2 is consistent with the differing specific activation of the *Arthrobacter* enzyme by these cations (Smith et al., 1981).

unambiguously at this resolution. In both cases multiple bound states are possible.

Inhibition Studies. The inhibitory properties of DDIG and DDIM toward D-xylose isomerase were investigated so far as the limited quantities of material allowed. Four sets of conditions were possible for DDIG, and these indicated some competition with the substrate and a K_i of 50 mM. DDIM displayed markedly less inhibition of the enzyme with K_i at least 5 times that for DDIG. Due to the weak inhibition, it was not possible to measure competition of DDIM with the substrate. No reduction in activity was observed in the presence of AM at 200 mM.

Inhibition studies could not be carried out for TF and AB1 since only small amounts of these compounds were available.

DISCUSSION

The observed binding mode of DNJ to D-xylose isomerase serves to confirm the role of His53. By considering the inhibitor binding mode as a model for the aldose–enzyme complex, a number of conclusions may be drawn. The proximity of the imidazole of His53 to the imino group in

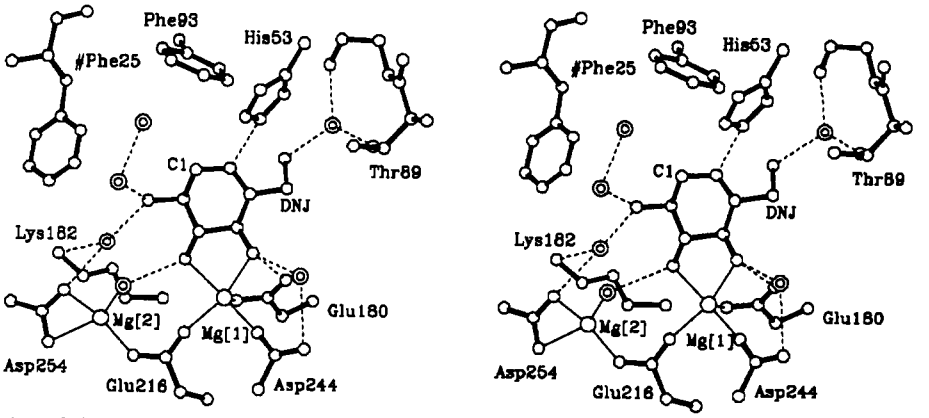

FIGURE 3: Stereodrawing of the DNJ–enzyme complex showing possible hydrogen bonds and metal ligation at the active site. Side chains of relevant residues are shown using dark lines. #Phe25 is from a neighboring subunit in the tetramer. Ordered solvent molecules are shown by double circles. Possible hydrogen bonds are shown using single dashed lines. Only part of the coordination shell of the metal sites is shown, and the bonds are indicated by single lines.

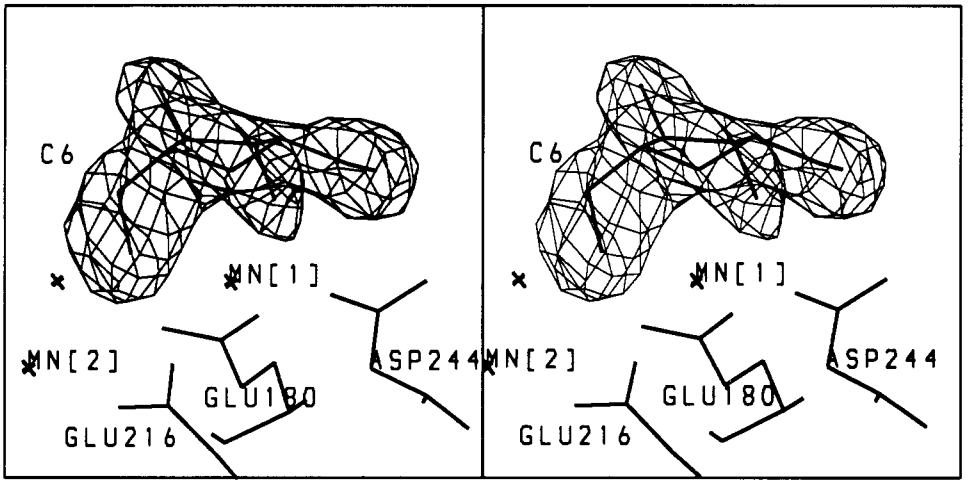

FIGURE 4: Stereodrawing of the electron density for active site region of the DDIG–enzyme complex. The electron density was calculated using Fourier coefficients $(F_o - F_c)$ and is contoured at 7σ. For the calculation of F_c and α, the coordinates of DDIG were omitted. The atomic model is shown using thick lines. The unlabeled crosses are ordered solvent molecules.

DNJ and its disposition relative to C1 are consistent with reactivity of the α- and not the β-pyranose form of the sugar. This binding mode for pyranose allows for a hydrogen transfer with a minimum of molecular motion. The cation at site 1 binds the pyranose and orients the substrate for the subsequent steps in the reaction. The imidazole group of His53 is polarized by Asp56 and catalyzes the ring opening of the α-pyranose sugar by transfer of the O1-hydroxyl hydrogen to O5 (Collyer et al., 1990; Lee et al., 1990; Whitlow et al., 1991).

If a β-pyranose is superposed onto the corresponding DNJ atomic positions, there is a steric clash. O1 of the aldose is, in this superposition, located less than 3 Å from the benzene groups of side chains Phe93 and Trp136. Any binding of a β-pyranose must be of a different conformation to that observed here for DNJ.

For the reverse process, the reaction with ketoses, the evidence for the anomeric specificity is indirect. Compounds which mimic the stereochemistry of the BDFF bind poorly to the enzyme; AM is not observed to inhibit, and DDIM shows evidence of binding only at concentrations greater than the K_m for D-fructose (Smith et al., 1991). This result supports the evidence presented by Makkee et al. (1984) for a preference by the enzyme for ADFF over BDFF.

There is little evidence with which to measure the relative reactivity of the furanose and open-chain keto forms of the substrates. Aldehydo forms of the sugars are not present in significant concentrations, but the keto forms of D-xylulose and D-fructose are more abundant (Angyal, 1984). The fraction of the keto form in D-fructose is observed to be 0.8% in D_2O at 31 °C (Wolff & Breitmaier, 1979). The open-chain sugar analogues xylitol and D-sorbitol do compete potently for substrate (Smith et al., 1991) and bind in an extended open-chain conformation to the enzyme (Henrick et al., 1989). This extended open-chain conformation is also observed when crystals are equilibrated with substrate, suggesting that keto and aldehydo forms are present as part of the reaction pathway (Collyer et al., 1990; Whitlow et al., 1991). A hypothesis consistent with the kinetic data is that the enzyme binds to and reacts with both the cyclic ADFF and open-chain keto D-fructose.

The relevance of this hypothesis to the specificity of D-xylose isomerase toward its physiological substrate D-xylulose is uncertain. As much as 22% of total D-xylulose in D_2O at 37 °C is present in the open-chain keto form (Angyal et al., 1976). In this case, where a substantial fraction of the sugar is present in the open-chain keto form, the keto form may be the dominant reacting species.

There is less structural knowledge of the binding of ADFF than for the open-chain keto form. The inhibitor DDIG does compete with substrate, but the crystal structure of the complex DDIG cannot be simply interpreted as a model for an ADFF–enzyme complex. If an ADFF is superimposed onto the corresonding DDIG atomic positions, there is a steric clash. O2 of the ketose is located, in this superposition, less than 3

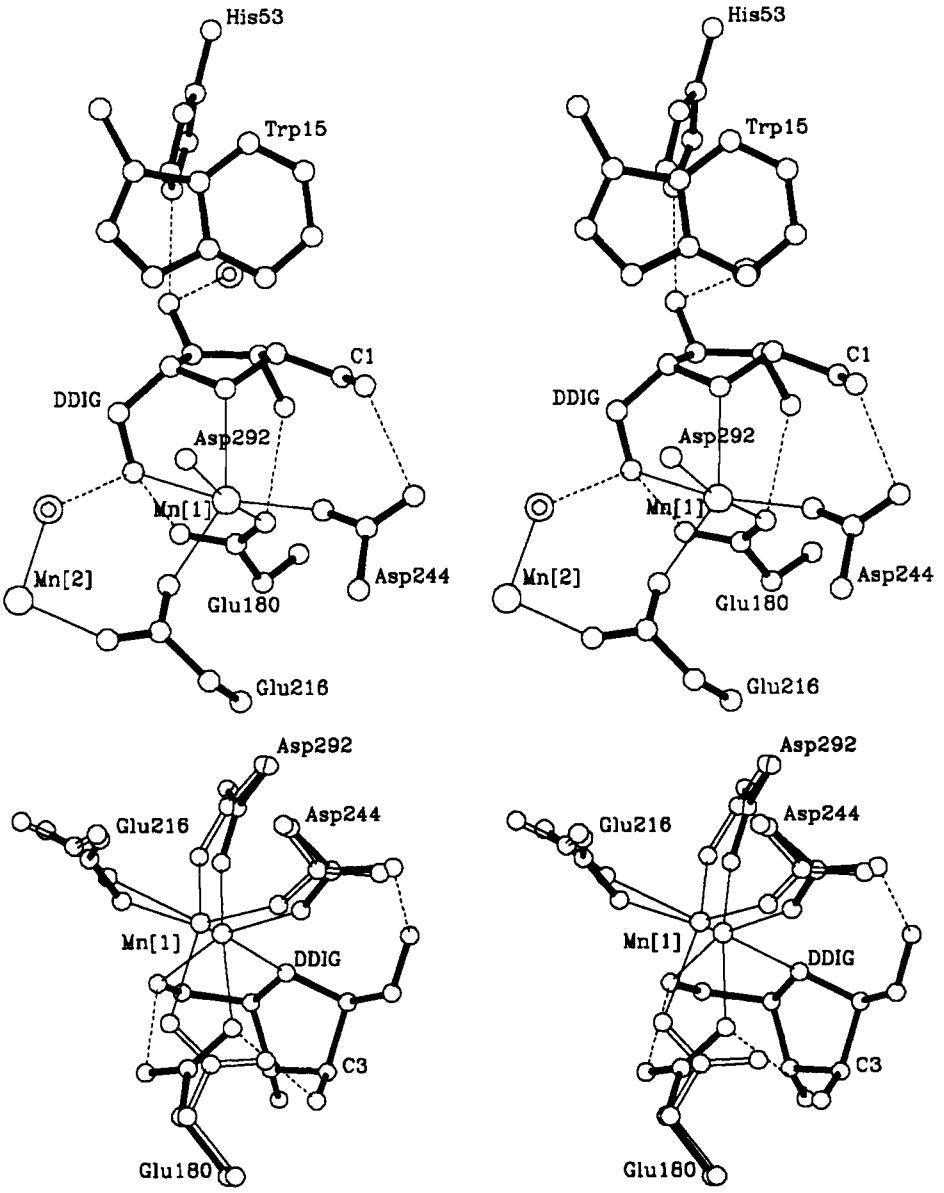

FIGURE 5: Stereodrawing of DDIG–enzyme complex showing possible hydrogen bonds and metal ligation at the active site. Side chains of relevant residues are shown using dark lines. Ordered solvent molecules are shown by double circles. Possible hydrogen bonds are shown using single dashed lines. Cation to ligand bonds are indicated by single lines. (a, top) Cut-away view of the binding pocket indicating the juxtaposition of C6 in the inhibitor to cation sites 1 and 2. Only one oxygen of Asp292 is shown. (b, bottom) Second view showing the bonds near cation site 1. Only part of the coordination shell of cation site 1 is shown. Superposed is the "normal" structure of site 1; this example is the 5-thioglucose–enzyme complex (Collyer et al., 1990) and is shown using clear lines. The carbon α-positions in the two structures were superposed to a rms agreement of 0.2 Å.

Å from the benzene group of side chain Trp15 (Figure 5a).

A β-furanose moiety has been observed crystallographically bound at the active site of the enzyme following covalent modification by, and isomerization of, 3-deoxy-3-fluoromethylene-D-glucose (Carrell et al., 1989). The BDFF group is bound covalently via the methylene group on C3 to the imidazole of the equivalent of His53. Like the imino group of the DDIG complex reported here, the ring oxygen of the furanose binds to the cation at site 1. The hydroxyl on C1 also is a ligand of the cation at site 1 in the same way as the O6 of DDIG (Table III). In fact, the set of cation to sugar bonds and hydrogen bonds which contribute to the stability of the covalently bound furanose are almost symmetrically related to the set of interactions listed here in Table III for DDIG.

BDFF has a pseudo-2-fold axis of symmetry (not obeyed by O2) about a line passing through the ring oxygen and the C3–C4 bond. If BDFF is approximately overlayed with the observed DDIG atomic positions, and then rotated 180° about the axis, a model is produced in which BDFF is bound in a manner very similar to the furanose observed by Carrell et al. (1989).

If the operation is repeated with the reactive anomer ADFF, a similar model is made and is shown in Figure 6. In such a model, the sugar ligates to the cation at site 1 via the ring oxygen and the anomeric hydroxyl at C2. This model has a number of features consistent with it being a putative productive binding mode for ketoses:

(1) Evidence presented here and elsewhere (Makkee et al., 1984) indicates that the α-D-furanose anomer is reactive.

(2) The atomic positions in this model are approximately related by the pseudosymmetry of the sugar to the crystallographically observed atomic positions of an inhibitor of the enzyme. The structure of the DDIG–enzyme complex reported here is the template for this model. This DDIG complex cannot be interpreted by simple superposition as a

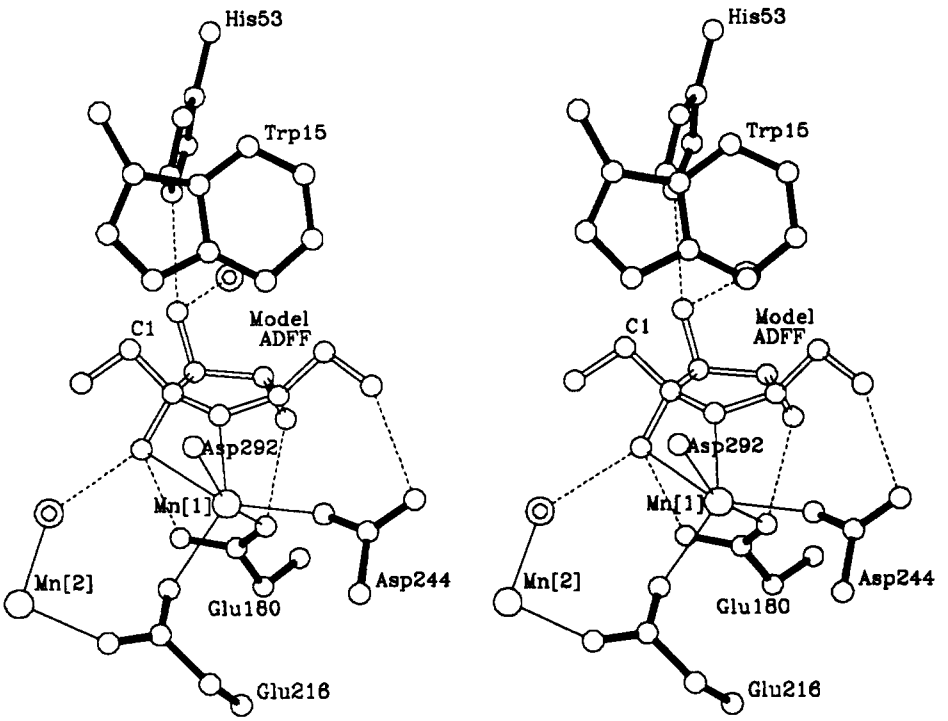

FIGURE 6: Stereodrawing of enzyme active site showing a proposed model for an ADFF–enzyme complex. Side chains of relevant residues are shown using dark lines. Ordered solvent molecules are shown by double circles. Possible hydrogen bonds are shown using single dashed lines. Cation to ligand bonds are indicated by single lines. Only one oxygen of Asp292 is shown. The juxtaposition of C1 in the ADFF–enzyme model to the cation sites is indicated. ADFF is shown using clear lines.

model for substrate binding, but the pseudosymmetry allows for a sterochemically sensible interpretation.

(3) The set of cation to sugar bonds in this proposed model mimics those observed crystallographically for covalently bound fructose (Carrell et al., 1989).

(4) In the model, a base (Wat519) is conveniently within hydrogen-bonding distance of the anomeric oxygen O2 and thus may facilitate sugar ring opening. The basic water molecule Wat519 bound to the cation at site 2 is close to O2 (Figure 6) and may act as a base to convert the α-D-furanose anomer into the reactive keto form. The ring oxygen O5 is a ligand of cation site 1.

(5) This model would explain the lack of reactivity for a β-D-furanose. If a β-D-furanose bound in this way, the anomeric oxygen at C2 would not be located within hydrogen-bonding distance of a base.

(6) The juxtaposition of C1–C2 to the active site of the enzyme in this proposed fructose conformation is the same as that observed for other inhibitors and substrates reported here and elsewhere (Henrick et al., 1989; Collyer et al., 1990; Whitlow et al., 1991). The proposal puts the sugar in an orientation consistent with the established mechanism for isomerization, with the furanose ring in a completely different orientation to that observed for pyranoses.

The use of deoxysugars as probes enables structures of sugar–enzyme complexes to be visualized by analogy. The binding affinity of a nonphysiological substrate of D-xylose isomerase has been improved (Meng et al., 1991), and structural information can guide this work, leading to a better understanding of the reaction mechanism.

ACKNOWLEDGMENT

We thank Dr. R. Nash, Jodrell Laboratory, Royal Botanic Gardens Kew and Bayer AG for samples of deoxysugars, J. Akins for protein purification, and Synchrotron Radiation Source, Daresbury, U.K., for the provision of synchrotron facilities.

REFERENCES

Akins, J., Brick, P., Jones, H. B., Hirayama, N., Shaw, P.-C., & Blow, D. M. (1986) *Biochim. Biophys. Acta 874*, 375–377.

Angyal, S. J. (1984) *Adv. Carbohydr. Chem. Biochem. 42*, 15–68.

Angyal, S. J., Bethell, G. S., Cowley, D. E., & Pickles, V. A. (1976) *Aust. J. Chem. 29*, 1239–1247.

Batt, C. A., Jamieson, A. C., & Vandeyar, M. A. (1989) *Proc. Natl. Acad. Sci. U.S.A. 87*, 618–622.

Blow, D. M., Birktoft, J. J., & Hartley, B. S. (1969) *Nature 221*, 337–340.

Bock, K., Meldal, M., Meyer, B., & Wiebe, L. (1983) *Acta Chem. Scand. B37*, 101–108.

Carrell, H. L., Glusker, J. P., Burger, V., Manfre, F., Tritsch, D., & Biellmann, J.-F. (1989) *Proc. Natl. Acad. Sci. U.S.A. 86*, 4440–4444.

Chmielewski, M., & Whistler, R. L. (1975) *J. Org. Chem. 40*, 639–643.

Collyer, C. A., & Blow, D. M. (1990) *Proc. Natl. Acad. Sci. U.S.A. 87*, 1362–1366.

Collyer, C. A., Henrick, K., & Blow, D. M. (1990) *J. Mol. Biol. 212*, 211–235.

Feather, M. S., Deshpande, V., & Lybyer, M. J. (1970) *Biochem. Biophys. Res. Commun. 38*, 859–863.

Fleet, G. W. J., & Smith, P. W. (1985) *Tetrahedron Lett. 26*, 1469–1472.

Goux, W. J. (1985) *J. Am. Chem. Soc. 107*, 4320–4327.

Hendrickson, W. A., & Konnert, J. H. (1980) in *Computing in Crystallography* (Diamond, R., Ramesseshan, S., & Venkatesan, K., Eds.) pp 1301–1323, Indian Academy of Sciences, Bangalore, India.

Henrick, K., Blow, D. M., Carrell, H. L., & Glusker, J. P. (1987) *Protein Eng. 1*, 467–469.

Henrick, K., Collyer, C. A., & Blow, D. M. (1989) *J. Mol. Biol. 208*, 129–157.

Inouye, S., Tsuruoka, T., Ito, T., & Niida, T. (1968) *Tetrahedron 24*, 2125–2144.
Lee, C., Bagdasarian, M., Meng, M., & Zeikus, J. G. (1990) *J. Biol. Chem. 265*, 19082–19090.
Makkee, M., Kieboom, A. P. G., & van Bekkum, H. (1984) *Recl. Trav. Chim. Pays-Bas 103*, 361–364.
McKay, G. A., & Tavlarides, L. L. (1979) *J. Mol. Catal. 6*, 57–69.
Meng, M., Lee, C., Bagdasarian, M., & Zeikus, J. G. (1991) *Proc. Natl. Acad. Sci. U.S.A. 88*, 4015–4019.
Nash, R. J., Bell, E. A., & Williams, J. M. (1985) *Phytochemistry 24*, 1620–1622.
Patil, J. R., & Bose, J. L. (1966) *J. Indian Chem. Soc. 43*, 161–168.
Rangarajan, M., & Hartley, B. S. (1992) *Biochem. J. 283*, 223–233.
Reitz, A. B., & Baxter, E. W. (1990) *Tetrahedron Lett. 31*, 6777–6790.
Schray, K. J., & Rose, I. A. (1971) *Biochemistry 10*, 1058–1062.
Schray, K. J., & Mildvan, A. S. (1972) *J. Biol. Chem. 247*, 2034–2037.
Smith, C. A., Rangarajan, M., & Hartley, B. S. (1991) *Biochem. J. 277*, 255–261.
Whitlow, M., Howard, A. J., Finzel, B. C., Poulos, T. L., Winborne, E., & Gilliland, G. L. (1991) *Proteins 9*, 153–173.
Wolff, G. J., & Breitmaier, E. (1979) *Chem.-Ztg. 103*, 232–233.
Wyn, D., Jones, C., Nash, R. J., Bell, E. A., & Williams, J. M. (1985) *Tetrahedron Lett. 26*, 3125–3126.
Young, J. M., Schray, K. J., & Mildvan, A. S. (1975) *J. Biol. Chem. 250*, 9021–9027.

Registry No. DNJ, 19130-96-2; DDIG, 132295-44-4; His, 71-00-1; Mg^{2+}, 7439-95-4; Mn^{2+}, 7439-96-5; ADFF, 10489-79-9; AB1, 100937-52-8; TF, 53821-50-4; DDIM, 59920-31-9; H_2O, 7732-18-5; D-xylose isomerase, 9023-82-9.